

# Low-energy inter-band Kondo bound states in orbital-selective Mott phases

Jia-Ming Wang,<sup>1,2,\*</sup> Yin Chen,<sup>1,2,\*</sup> Yi-Heng Tian,<sup>1,2,\*</sup> Rong-Qiang He,<sup>1,2,†</sup> and Zhong-Yi Lu<sup>1,2,3,‡</sup>

<sup>1</sup>*Department of Physics, Renmin University of China, Beijing 100872, China*

<sup>2</sup>*Key Laboratory of Quantum State Construction and Manipulation (Ministry of Education), Renmin University of China, Beijing 100872, China*

<sup>3</sup>*Hefei National Laboratory, Hefei 230088, China*

(Dated: July 23, 2024)

Low-energy excitations may manifest intricate behaviors of correlated electron systems and provide essential insights into the dynamics of quantum states and phase transitions. We study a two-orbital Hubbard model featuring the so-called holon-doublon low-energy excitations in the Mott insulating narrow band in the orbital-selective Mott phase (OSMP). We employ an improved dynamical mean-field theory (DMFT) technique to calculate the spectral functions at zero temperature. We show that the holon-doublon bound state is not the sole component of the low-energy excitations. Instead, it should be a bound state composed of a Kondo-like state in the wide band and a doublon in the narrow band, named inter-band Kondo-like (IBK) bound states. Notably, as the bandwidths of the two bands approach each other, we find anomalous IBK bound-state excitations in the metallic *wide* band.

The Mott transition, which indicates the transformation from metallic to insulating states driven by strong electron interactions, is a pivotal phenomenon in condensed matter physics [1, 2]. When a metallic system undergoes a Mott transition, it enters a Mott phase. In multi-orbital systems with varying bandwidths, the phase that some bands are Mott insulating while the others remain metallic is known as the orbital-selective Mott phase (OSMP) [3, 4]. This phenomenon was initially discussed widely in theoretical studies [5–9]. Recently, it has been found experimentally in some materials [10–14].

In earlier years, research on low-energy excitations near Mott transitions was limited to single-band Hubbard models [15, 16]. Recently, Núñez-Fernández *et al.* [17] studied a half-filled two-orbital Hubbard model,

$$H = - \sum_{\langle ij \rangle, l, \sigma} t_l c_{i l \sigma}^\dagger c_{j l \sigma} + U \sum_{i, l} (n_{i l \uparrow} - \frac{1}{2})(n_{i l \downarrow} - \frac{1}{2}) + U' \sum_i (n_{i 1} - 1)(n_{i 2} - 1), \quad (1)$$

where  $c_{i l \sigma}^\dagger$  and  $c_{i l \sigma}$  are the electron creation and annihilation operators for orbital  $l$  on site  $i$  with spin  $\sigma$ ,  $U$  ( $U'$ ) is the intra- (inter-)orbital Coulomb repulsion,  $n_{i l \sigma} = c_{i l \sigma}^\dagger c_{i l \sigma}$ ,  $n_{i l} = \sum_\sigma n_{i l \sigma}$ , and  $\langle ij \rangle$  indicates that only the nearest-neighbor hoppings are considered. In this model,  $l = 1, 2$  also denote the wide band (WB) and narrow band (NB), respectively, namely  $t_1 > t_2$ . As  $U$  increases, with  $\Delta = U - U' > 0$ , the NB first transitions into a Mott insulating state, while the WB remains metallic, indicating that the system has entered an OSMP. This is illustrated in Fig. 1(a). Núñez-Fernández *et al.* [17] identified new quasiparticle (QP) states. In the OSMP, these QP peaks persist as in-gap states within the Mott gap of the insulating NB around  $\omega = \pm\Delta$ . They also introduced the concept of the holon-doublon (HD) bound state, in which a doublon in the NB binds with

a holon in the WB. They proposed that the QPs are mainly formed by the HD bound states at  $\omega = \pm\Delta$ . At the symmetric point  $\Delta = 0$  ( $U = U'$ ), the QP peaks are located at the Fermi energy, leading to a simultaneous Mott transition in the two band even if the bandwidths are different.

The discovery of the HD bound state inspired subsequent research on low-energy excitations in two-orbital systems. Niu *et al.* [18] studied a Kanamori model, which extends the two-orbital Hubbard model in Eq. (1) by adding spin-flip and pair-hopping Hund interactions, and found similar QPs. Hallberg *et al.* [19] studied a hole-doped system and observed that the Hund's coupling splits the HD excitation peaks. Subsequent studies using different numerical methods, such as the slave-spin method [20], numerical renormalization group [21], and density matrix renormalization group [22–24], have also found the QPs. Currently, theoretical studies of the low-energy excitations in the OSMP seem to be comprehensive, agreeing that the HD bound states are the main forms of the low-energy excitations [17–24]. However, we will show that this picture is incomplete or even wrong.

In this Letter, we use an improved dynamical mean-field theory (DMFT) technique, incorporating the natural orbitals renormalization group (NORG) as the impurity solver [25–28], to study the low-energy excitation behavior of the two-orbital model (1). By calculating the density of states (DOS) and special Green's functions, we find previously undetected components of the low-energy excitations in the Mott insulating narrow band. These components help us better understand the formation of QP peaks and reveal that the Kondo-like state in the WB is binding a doublon in the NB for the excitation states at  $\omega = \pm\Delta$ . We name these low-energy excitation states inter-band Kondo-like (IBK) bound states. Additionally, as the two orbitals' bandwidths approach each other, we have observed two anomalous IBK bound states

around  $\omega = \pm 2\Delta$  in the WB.

*Model and method.* We consider the half-filled two-orbital Hubbard model, described by Eq. (1), on a Bethe lattice with infinite coordination number [29], resulting in a half-bandwidth of  $D_l = 2t_l$ . We set  $t_1 = 0.5$ , resulting in the WB's half-bandwidth  $D_1 = 1$ , which we adopt as the energy unit. We utilize DMFT with NORG to study this model. For technical details, see the Supplementary Material [28].

In Fig. 1(a), we present the DOS, demonstrating that the NB becomes insulating while the WB remains metallic, indicating that the system enters an OSMP under certain conditions ( $U = 3$ ,  $\Delta = 0.3$ , and  $t_2 = 0.1t_1$ ). Notably, the WB exhibits a Kondo-like QP peak around  $\omega = 0$ , while the NB has two low-energy QP peaks around  $\omega = \pm\Delta$ .

To further clarify the nature of the low-energy excitations, we define and calculate the special Green's func-

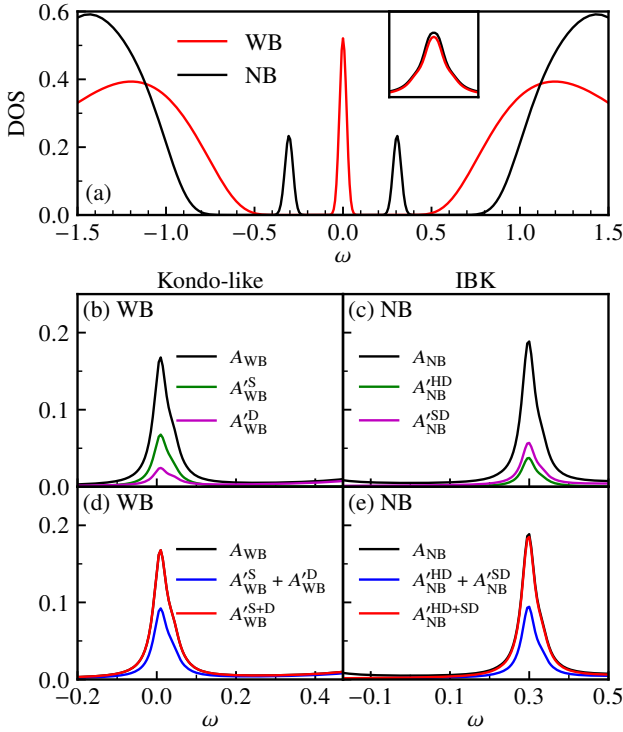


FIG. 1. (a) DOS for the two-orbital model with  $U = 3$ ,  $\Delta = 0.3$ , and  $t_2 = 0.1t_1$ . In the WB, a prominent Kondo-like QP peak is evident around the Fermi level, and in the NB, two distinct QP peaks are visible around  $\omega = \pm\Delta$ . Inset: The total spectral weight of the two peaks around  $\omega = \pm\Delta$  in the NB matches the total spectral weight of the Kondo-like QP peak in the WB. Unraveling the excitation spectra in the WB and NB (b-e), and comparing with the standard Green's function,  $A \equiv -\frac{1}{\pi}\text{Im}G^>$ . Individual special Green's functions (b)  $A'^S_{WB}$  and  $A'^D_{WB}$ ; (c)  $A'^{HD}_{NB}$  and  $A'^{SD}_{NB}$ . Combined special Green's functions (d)  $A'^S_{WB} + A'^D_{WB}$  and  $A'^{S+D}_{WB}$ ; (e)  $A'^{HD}_{NB} + A'^{SD}_{NB}$  and  $A'^{HD+SD}_{NB}$ . See the text for details.

tions to unravel the spectral function:

$$\begin{aligned} A'(\omega) &\equiv -\frac{1}{\pi}\text{Im}G'^>(\omega) \\ &= -\frac{1}{\pi}\text{Im}\langle\phi|(\omega + i\eta - H_{\text{imp}})^{-1}|\phi\rangle, \end{aligned} \quad (2)$$

where  $|\phi\rangle$  is a single-particle excitation state and  $H_{\text{imp}}$  is the mapped impurity model's Hamiltonian from DMFT (for details, see the Supplementary Material [28]). For the excitations in the NB,  $|\phi\rangle$  can be one of the following states:

$$\begin{cases} |\phi_{\text{NB}}^{\text{HD}}\rangle &= (1 - n_{1\uparrow})(1 - n_{1\downarrow})n_{2\downarrow}c_{2\uparrow}^\dagger|\text{gs}\rangle, \\ |\phi_{\text{NB}}^{\text{SD}}\rangle &= n_{1\uparrow}(1 - n_{1\downarrow})n_{2\downarrow}c_{2\uparrow}^\dagger|\text{gs}\rangle \\ &+ (1 - n_{1\uparrow})n_{1\downarrow}n_{2\downarrow}c_{2\uparrow}^\dagger|\text{gs}\rangle, \\ |\phi_{\text{NB}}^{\text{DD}}\rangle &= n_{1\uparrow}n_{1\downarrow}n_{2\downarrow}c_{2\uparrow}^\dagger|\text{gs}\rangle, \end{cases} \quad (3)$$

where  $|\text{gs}\rangle$  refers to the ground state of the impurity model,  $c_{l\sigma}^\dagger$  is the electron creation operator for the impurity orbital  $l$  with spin  $\sigma$ , and  $n_{l\sigma} = c_{l\sigma}^\dagger c_{l\sigma}$ . The impurity orbital of the NB, after inserting a particle, becomes mainly doubly occupied, and the impurity orbital of the WB may be empty ( $|\phi_{\text{NB}}^{\text{HD}}\rangle$ ), singly occupied ( $|\phi_{\text{NB}}^{\text{SD}}\rangle$ ), or doubly occupied ( $|\phi_{\text{NB}}^{\text{DD}}\rangle$ ). Noting that  $|\phi_{\text{NB}}^{\text{HD}}\rangle + |\phi_{\text{NB}}^{\text{SD}}\rangle + |\phi_{\text{NB}}^{\text{DD}}\rangle = n_{2\downarrow}c_{2\uparrow}^\dagger|\text{gs}\rangle$ , with a doublon in the NB.

*Kondo-like excitations.* The WB exhibits a Kondo-like QP peak around  $\omega = 0$ , as shown in Fig. 1(a). We unravel the DOS for the WB using Eq. (2). In Fig. 1(b),  $A_{\text{WB}}$  represents the standard Green's function,  $A_{\text{WB}} \equiv -\frac{1}{\pi}\text{Im}G_{\text{WB}}^>$ .  $A'^S_{\text{WB}}$  and  $A'^D_{\text{WB}}$  are the special Green's functions that correspond to the particle excitation states with single occupancy  $|\phi_{\text{WB}}^{\text{S}}\rangle = (1 - n_{1\downarrow})c_{1\uparrow}^\dagger|\text{gs}\rangle$  and double occupancy  $|\phi_{\text{WB}}^{\text{D}}\rangle = n_{1\downarrow}c_{1\uparrow}^\dagger|\text{gs}\rangle$  in the WB, respectively. We have observed that both  $A'^S_{\text{WB}}$  and  $A'^D_{\text{WB}}$  are nonzero around  $\omega = 0$ . This indicates that the particle excitation state has contributions from both the  $|\phi_{\text{WB}}^{\text{S}}\rangle$  and  $|\phi_{\text{WB}}^{\text{D}}\rangle$  components. In Fig. 1(d), we introduce a special Green's function  $A'^{S+D}_{\text{WB}}$  with  $|\phi\rangle = |\phi_{\text{WB}}^{\text{S}}\rangle + |\phi_{\text{WB}}^{\text{D}}\rangle$  in Eq. (2) and compare it with  $A_{\text{WB}}$  and the sum  $A'^S_{\text{WB}} + A'^D_{\text{WB}}$ . We find that  $A'^{S+D}_{\text{WB}}$  matches  $A_{\text{WB}}$ , while  $A'^S_{\text{WB}} + A'^D_{\text{WB}}$  does not. The difference between the two is that the off-diagonal parts,  $\langle\phi_{\text{WB}}^{\text{S}}|(\omega + i\eta - H_{\text{imp}})^{-1}|\phi_{\text{WB}}^{\text{D}}\rangle$  and  $\langle\phi_{\text{WB}}^{\text{D}}|(\omega + i\eta - H_{\text{imp}})^{-1}|\phi_{\text{WB}}^{\text{S}}\rangle$ , are present in the former but missing in the latter. This shows that the Kondo-like particle excitation state is a superposition state of the singly and doubly occupied states in the WB.

*IBK bound states.* We show the calculated the special Green's functions of the NB (Eq. (2)) in Fig. 1(c). Surprisingly, in addition to an HD component around  $\omega = \Delta$ , an SD component is also identified. This shows that the HD component alone is insufficient to account for the low-energy excitation. Thus, this low-energy excitation is not an HD bound state (with a localized holon in the WB and a localized doublon in

the NB). To further unravel this excitation, we introduce a special Green's function  $A_{\text{NB}}^{\text{HD+SD}}$  with  $|\phi\rangle = |\phi_{\text{NB}}^{\text{HD}}\rangle + |\phi_{\text{NB}}^{\text{SD}}\rangle$  in Eq. (2) and compare it with  $A_{\text{NB}}^{\text{HD}} + A_{\text{NB}}^{\text{SD}}$  and  $A_{\text{NB}} \equiv -\frac{1}{\pi}\text{Im}G_{\text{NB}}^>$  in Fig. 1(e).  $A_{\text{NB}}^{\text{HD+SD}}$  perfectly matches  $A_{\text{NB}}$ , while the sum  $A_{\text{NB}}^{\text{HD}} + A_{\text{NB}}^{\text{SD}}$  does not. The difference between the two is that the off-diagonal parts,  $\langle\phi_{\text{NB}}^{\text{SD}}|(\omega + i\eta - H_{\text{imp}})^{-1}|\phi_{\text{NB}}^{\text{HD}}\rangle$  and  $\langle\phi_{\text{NB}}^{\text{HD}}|(\omega + i\eta - H_{\text{imp}})^{-1}|\phi_{\text{NB}}^{\text{SD}}\rangle$ , are present in the former but missing in the latter. Therefore, in the low-energy excitation state, the impurity orbital of the WB is neither in a localized holon state nor in a localized single-occupancy state, but rather in a superposition state involving both the impurity and the bath, noting that the WB itself is particle-number conserved. It turns out that the NB is in a localized doublon state, while the WB is not in a localized state involving only the impurity orbital. Additionally, the inset of Fig. 1(a) shows that the total spectral weight of the two NB's QP peaks around  $\omega = \pm\Delta$  is approximately equal to the spectral weight of the Kondo-like QP peak around the Fermi level. We name the excitation states around  $\omega = \pm\Delta$  in the NB inter-band Kondo-like (IBK) bound states.

We use a Bethe lattice with a coordination number of two to further explain the key features of an IBK bound state in the OSMP, with a schematic of this state shown in Fig. 2(a). Inserting an electron into the orbital on the middle site in the NB leads to a doublon in the NB, binding with an empty state in the metallic WB, creating an HD component, as depicted in the right part of Fig. 2(a). The interaction potential energy of the HD component is only  $\Delta$  higher than that of the ground state

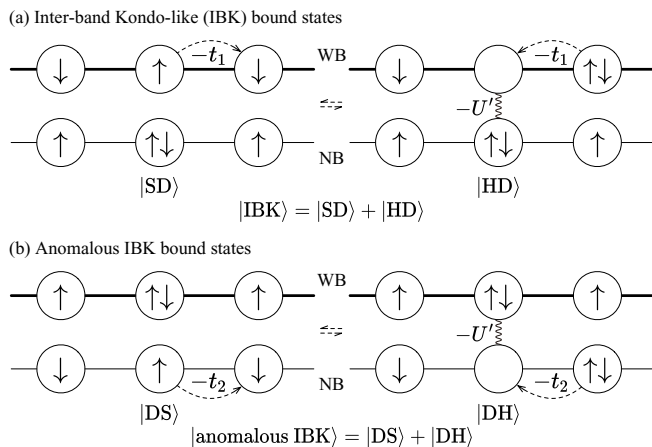


FIG. 2. Schematic diagrams of the IBK bound states (a) and the anomalous IBK bound states (b). In these diagrams, the WB are represented by thicker lines, while the NB are depicted with thinner lines, indicating their respective hopping integrals,  $-t_1$  for WB and  $-t_2$  for NB. For the (anomalous) IBK bound states, the existence of an HD (DH) excitation state allows the system to reduce its  $U'$  energy cost. The double arrow indicates that the SD and HD (DS and DH) states form superposition states.

and is less than the interaction potential energies of the SD and the DD components. More specifically, as described in Eq. (1), the interaction potential energy for the middle orbital of the HD component is  $\frac{1}{4}U$  for both the wide and narrow bands, and  $-U'$  for the inter-orbital part. Comparing this to the ground-state potential energy of the middle site, which is  $-\frac{1}{4}U$  because of single occupancy in both the WB and NB, we find that the energy gap between the HD component and the ground state is  $\Delta = U - U'$ . In contrast, the energy gap between the DD (SD) component and the ground state is  $U + U'$  ( $\frac{1}{2}U$ ). Noting that the DD component is much higher than  $\Delta$ , this excludes the DD component from the low-energy excitation states.

Since the WB is close to the Mott transition, the kinetic energy in the WB is comparable to the potential energy. This makes the empty state in the orbital on the middle site of the WB, namely the holon in the WB, is unstable. This instability allows an electron to appear at the middle site in the WB, leading to the existence of an SD component, as depicted in the left part of Fig. 2(a). The nonzero off-diagonal contributions (e.g.,  $\langle\phi_{\text{NB}}^{\text{SD}}|(\omega + i\eta - H_{\text{imp}})^{-1}|\phi_{\text{NB}}^{\text{HD}}\rangle \neq 0$ ) demonstrate that an IBK bound state is a superposition of empty and singly occupied states in the WB with a doublon in the NB, as marked by the middle double arrow in Fig. 2(a). The interplay between intra- and inter-orbital interactions results in the IBK bound states being  $\Delta$  higher in energy than the ground state. However, the Kondo-like state in the WB is not produced by a single-particle excitation in the WB but by a single-particle excitation in the NB. For this excitation state, the inter-band interaction  $U'$  plays a key role.

*Anomalous IBK bound states.* We consider another scenario where the bandwidths of the two-orbital model (1) approach each other. In Fig. 3(a), we present the DOS with  $t_2 = 0.8t_1$ ,  $U = 3.3$ , and  $\Delta = 0.2$ . The WB exhibits a Kondo-like QP peak around  $\omega = 0$ , while the NB has two IBK QP peaks around  $\omega = \pm\Delta$ , similar to what we discussed above for the normal IBK bound state. Unexpectedly, in Fig. 3(a), we have observed additional QP peaks around  $\omega = \pm 2\Delta$  in the WB, distinct from the Kondo-like QP peak around the Fermi level. To confirm these additional QP peaks, we calculate the DOS with different  $\Delta$  while keeping other parameters fixed. In Fig. 4, we show the dependence of the QP peaks with  $\Delta$  in both the NB and WB. The IBK bound states in the NB are observed around  $\omega = \pm\Delta$ , as shown in Fig. 4(a). In Fig. 4(b), besides the Kondo-like QP peak, we observe additional QP peaks in the WB around  $\omega = \pm 2\Delta$ .

To understand the additional excitation peaks at  $\omega = \pm 2\Delta$ , we applied a similar analysis used for the IBK bound states in the NB and calculated the special Green's functions  $A_{\text{WB}}$ ,  $A_{\text{WB}}^{\text{DH}}$ ,  $A_{\text{WB}}^{\text{DS}}$ , and  $A_{\text{WB}}^{\text{DH+DS}}$  as described in Eq. (2). The impurity orbital of the WB, after inserting a particle, becomes mainly doubly occu-

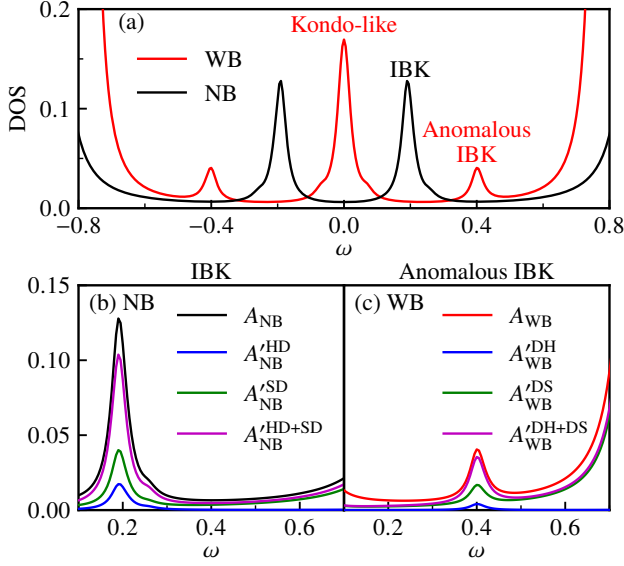


FIG. 3. (a) DOS for the two-orbital model with  $U = 3.3$ ,  $\Delta = 0.2$ , and  $t_2 = 0.8t_1$ . Unraveling the excitation spectra in the NB and WB (b-c), and comparing with the standard Green's function,  $A \equiv -\frac{1}{\pi}\text{Im}G^>$ . (b) NB's special Green's functions  $A_{\text{NB}}^{\text{HD}}$ ,  $A_{\text{NB}}^{\text{SD}}$ , and  $A_{\text{NB}}^{\text{HD+SD}}$ . (c) WB's special Green's functions  $A_{\text{WB}}^{\text{DH}}$ ,  $A_{\text{WB}}^{\text{DS}}$ , and  $A_{\text{WB}}^{\text{DH+DS}}$ . See the text for details.

pie. The impurity orbital of the NB may be empty ( $|\phi_{\text{WB}}^{\text{DH}}\rangle = (1 - n_{2\uparrow})(1 - n_{2\downarrow})n_{1\downarrow}c_{1\uparrow}^\dagger |\text{gs}\rangle$ ), singly occupied ( $|\phi_{\text{WB}}^{\text{DS}}\rangle = n_{2\uparrow}(1 - n_{2\downarrow})n_{1\downarrow}c_{1\uparrow}^\dagger |\text{gs}\rangle + (1 - n_{2\uparrow})n_{2\downarrow}n_{1\downarrow}c_{1\uparrow}^\dagger$ ), or doubly occupied ( $|\phi_{\text{WB}}^{\text{DD}}\rangle = n_{2\uparrow}n_{2\downarrow}n_{1\downarrow}c_{1\uparrow}^\dagger$ ). Note that  $|\phi_{\text{WB}}^{\text{DH}}\rangle + |\phi_{\text{WB}}^{\text{DS}}\rangle + |\phi_{\text{WB}}^{\text{DD}}\rangle = n_{1\downarrow}c_{1\uparrow}^\dagger |\text{gs}\rangle$ , with a doublon in the WB. We compare these special Green's functions with the standard Green's function  $A_{\text{WB}}$ . As shown in Fig. 3(c), both  $A_{\text{WB}}^{\text{DH}}$  and  $A_{\text{WB}}^{\text{DS}}$  are nonzero at  $\omega = 2\Delta$ . The  $A_{\text{WB}}^{\text{DH+DS}}$  matches  $A_{\text{WB}}$ , while both  $A_{\text{WB}}^{\text{DH}}$  and  $A_{\text{WB}}^{\text{DS}}$  are less than  $A_{\text{WB}}$ . This indicates that the excitation state has off-diagonal contributions from both DS and DH components. Therefore, the impurity orbital of the NB is neither in a localized single-occupancy state nor in a localized holon state. Instead, it is in a superposition state involving both empty and singly occupied states, reminiscent of the IBK bound state in the NB discussed above. However, these states are quite anomalous, leading localized insulating NB states to have Kondo-like excitation states, which contradicts the typical characteristics of the localized Mott states. This shows that the particle excitation in the WB can affect the NB's localization and insulation in the anomalous IBK bound states.

To further explain the anomalous features of IBK bound states in the WB around  $\omega = \pm 2\Delta$ , we show a schematic of these states in Fig. 2(b). Inserting an electron into the orbital on the middle site in the WB leads to a doublon in the WB, binding with an empty state in the insulating NB, creating a DH component, as depicted

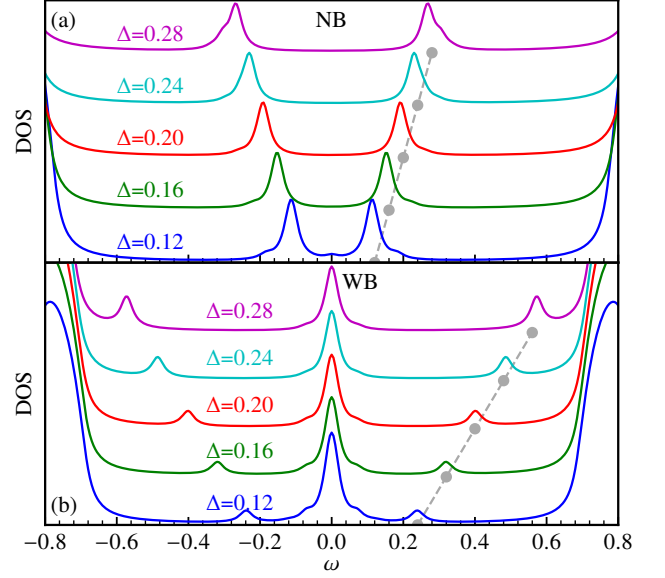


FIG. 4. Dependence of the IBK QP peak positions in the wide and narrow bands for  $U = 3.3$ ,  $t_2 = 0.8t_1$ . The IBK excitation peaks around  $\omega = 2\Delta$  in the wide band (a) and around  $\omega = \Delta$  in the narrow band (b) are shown. The grey dashed lines indicate the excitation peaks for each value of  $x = \Delta$  ( $\Delta = 0.12, 0.16, 0.20, 0.24, \text{ and } 0.28$ ).

in the right part of Fig. 2(b). The DH component gains an advantage in interaction potential energy for reasons similar to the HD component (discussed in normal IBK bound states in the NB). Since the NB is close to the Mott transition, the kinetic energy in the NB is comparable to the potential energy. This makes the empty state in the orbital on the middle site of the NB, namely the holon, unstable. This instability allows an electron to appear at the middle site in the NB, leading to the existence of an SD component, as depicted in the left part of Fig. 2(b). The nonzero off-diagonal contributions (e.g.,  $\langle \phi_{\text{NB}}^{\text{SD}} | (\omega + i\eta - H_{\text{imp}})^{-1} | \phi_{\text{NB}}^{\text{HD}} \rangle \neq 0$ ) demonstrate that an IBK bound state in the NB is a superposition of empty and singly occupied states with a doublon in the WB, as marked by the middle double arrow in Fig. 2(b). However, the position of the anomalous IBK QP peaks (around  $\omega = \pm 2\Delta$ ) cannot be explained by interaction potential energy, unlike the normal IBK, which is excited in the NB.

*Conclusion.* Using state-of-the-art numerical calculations for the two-orbital Hubbard model with a repulsive inter-orbital interaction, we have found that the IBK bound appearing in the Mott gap of the NB is a superposition of empty and singly occupied states in the WB with a doublon in the NB. This corrects the view of the HD bound state in the literature. When the bandwidths of the two orbitals approach each other, we have found anomalous IBK bound states around  $\omega = \pm 2\Delta$  in the WB. This discovery challenges the conventional under-

standing that the Mott insulating bands decouple from the other bands in an OSMP.

This work was supported by National Natural Science Foundation of China (Grant No. 11934020). Z.Y.L. was also supported by Innovation Program for Quantum Science and Technology (Grant No. 2021ZD0302402). Computational resources were provided by Physical Laboratory of High Performance Computing in Renmin University of China.

---

\* These authors contributed equally to this work.

† [rqhe@ruc.edu.cn](mailto:rqhe@ruc.edu.cn)

‡ [zlu@ruc.edu.cn](mailto:zlu@ruc.edu.cn)

- [1] N. F. Mott, Metal-insulator transition, *Rev. Mod. Phys.* **40**, 677 (1968).
- [2] M. Imada, A. Fujimori, and Y. Tokura, Metal-insulator transitions, *Rev. Mod. Phys.* **70**, 1039 (1998).
- [3] A. Koga, N. Kawakami, T. M. Rice, and M. Sigrist, Orbital-selective mott transitions in the degenerate hubbard model, *Phys. Rev. Lett.* **92**, 216402 (2004).
- [4] A. Liebsch, Novel mott transitions in a nonisotropic two-band hubbard model, *Phys. Rev. Lett.* **95**, 116402 (2005).
- [5] A. Koga, N. Kawakami, T. M. Rice, and M. Sigrist, Spin, charge, and orbital fluctuations in a multiorbital mott insulator, *Phys. Rev. B* **72**, 045128 (2005).
- [6] M. Ferrero, F. Becca, M. Fabrizio, and M. Capone, Dynamical behavior across the mott transition of two bands with different bandwidths, *Phys. Rev. B* **72**, 205126 (2005).
- [7] L. de' Medici, S. R. Hassan, M. Capone, and X. Dai, Orbital-selective mott transition out of band degeneracy lifting, *Phys. Rev. Lett.* **102**, 126401 (2009).
- [8] L. de' Medici, Hund's coupling and its key role in tuning multiorbital correlations, *Phys. Rev. B* **83**, 205112 (2011).
- [9] Z. Ouyang, R.-Q. He, and Z.-Y. Lu, *Dft+dmft study of correlated electronic structure in the monolayer-trilayer phase of La<sub>3</sub>Ni<sub>2</sub>O<sub>7</sub>* (2024), [arXiv:2407.08601](https://arxiv.org/abs/2407.08601) [cond-mat.str-el].
- [10] M. Vojta, Orbital-selective mott transitions: Heavy fermions and beyond, *Journal of Low Temperature Physics* **161**, 203 (2010).
- [11] T. Y. Xie, Z. Liu, C. Cao, Z. F. Wang, J. L. Yang, and W. Zhu, Microscopic theory of superconducting phase diagram in infinite-layer nickelates, *Phys. Rev. B* **106**, 035111 (2022).
- [12] M. Kim, S. Choi, W. H. Brito, and G. Kotliar, Orbital-selective mott transition effects and nontrivial topology of iron chalcogenide, *Phys. Rev. Lett.* **132**, 136504 (2024).
- [13] G. Cuono, R. M. Sattigeri, J. Skolimowski, and C. Autieri, Orbital-selective altermagnetism and correlation-enhanced spin-splitting in strongly-correlated transition metal oxides, *Journal of Magnetism and Magnetic Materials* **586**, 171163 (2023).
- [14] M. Horio, F. Forte, D. Sutter, M. Kim, C. G. Fatuzzo, C. E. Matt, S. Moser, T. Wada, V. Granata, R. Fittipaldi, Y. Sassa, G. Gatti, H. M. Rønnow, M. Hoesch, T. K. Kim, C. Jozwiak, A. Bostwick, E. Rotenberg, I. Matsuda, A. Georges, G. Sangiovanni, A. Vecchione, M. Cuoco, and J. Chang, Orbital-selective metal skin induced by alkali-metal-dosing mott-insulating Ca<sub>2</sub>RuO<sub>4</sub>, *Communications Physics* **6**, 323 (2023).
- [15] S. Zhou, Y. Wang, and Z. Wang, Doublon-holon binding, mott transition, and fractionalized antiferromagnet in the hubbard model, *Phys. Rev. B* **89**, 195119 (2014).
- [16] S.-S. B. Lee, J. von Delft, and A. Weichselbaum, Doublon-holon origin of the subpeaks at the hubbard band edges, *Phys. Rev. Lett.* **119**, 236402 (2017).
- [17] Y. Núñez Fernández, G. Kotliar, and K. Hallberg, Emergent low-energy bound states in the two-orbital hubbard model, *Phys. Rev. B* **97**, 121113 (2018).
- [18] Y. Niu, J. Sun, Y. Ni, J. Liu, Y. Song, and S. Feng, Doublon-holon excitations split by hund's rule coupling within the orbital-selective mott phase, *Phys. Rev. B* **100**, 075158 (2019).
- [19] K. Hallberg and Y. Núñez Fernández, Subbands in the doped two-orbital kanamori-hubbard model, *Phys. Rev. B* **102**, 245138 (2020).
- [20] Y. Komijani, K. Hallberg, and G. Kotliar, Renormalized dispersing multiplets in the spectrum of nearly mott localized systems, *Phys. Rev. B* **99**, 125150 (2019).
- [21] F. B. Kugler, S.-S. B. Lee, A. Weichselbaum, G. Kotliar, and J. von Delft, Orbital differentiation in hund metals, *Phys. Rev. B* **100**, 115159 (2019).
- [22] N. Aucar Boidi, H. Fernández García, Y. Núñez Fernández, and K. Hallberg, In-gap band in the one-dimensional two-orbital kanamori-hubbard model with interorbital coulomb interaction, *Phys. Rev. Res.* **3**, 043213 (2021).
- [23] M. Środa, J. Mravlje, G. Alvarez, E. Dagotto, and J. Herbrych, Hund bands in spectra of multiorbital systems, *Phys. Rev. B* **108**, L081102 (2023).
- [24] N. Aucar Boidi, A. P. Kampf, and K. Hallberg, Unconventional correlated metallic behavior due to interorbital coulomb interaction, *Phys. Rev. B* **109**, 085122 (2024).
- [25] R.-Q. He and Z.-Y. Lu, Quantum renormalization groups based on natural orbitals, *Phys. Rev. B* **89**, 085108 (2014).
- [26] R.-Q. He, J. Dai, and Z.-Y. Lu, Natural orbitals renormalization group approach to the two-impurity kondo critical point, *Phys. Rev. B* **91**, 155140 (2015).
- [27] R. Zheng, R.-Q. He, and Z.-Y. Lu, An anderson impurity interacting with the helical edge states in a quantum spin hall insulator, *Chinese Physics Letters* **35**, 067301 (2018).
- [28] See Supplemental Material at web, for (1) Method: dynamical mean-field theory, (2) Bath fitting on Matsubara frequency, (3) Solver: natural orbitals renormalization group, (4) Absence of orbital selective Mott transition. (5) Absence of orbital selective Mott transition.
- [29] A. Georges, G. Kotliar, W. Krauth, and M. J. Rozenberg, Dynamical mean-field theory of strongly correlated fermion systems and the limit of infinite dimensions, *Rev. Mod. Phys.* **68**, 13 (1996).